DALTON
PERSPECTIVE

The figure-of-eight twist to macrocycles: preorganization, self-organization and dynamics

Peter Comba,* Andreas Kühner and Alexander Peters

*Anorganisch-Chemisches Institut, Universität Heidelberg, Im Neuenheimer Feld 270,
69120 Heidelberg, Germany. Fax: +49 (6221) 54 66 17.
E-mail: comba@akcomba.oci.uni-heidelberg.de*

Received 3rd August 1998, Accepted 30th October 1998

Large macrocyclic rings (30- to 36-membered) with two dithiadiimine donor sets and two *para*- or *meta*-phenylene spacer groups undergo copper(I) induced folding with π stacking of the two benzene spacer groups. The type of folding (twisted to a helical or squeezed to an achiral macrocyclic shape) and the stability of the dicopper(I) compounds are analysed as a function of the ligand structure, the solid state structures, solution equilibria and dynamics and the comparison of the observed data with computed structures and conformational equilibria. Preliminary preparative studies suggest that derivatives with the observed structural motifs may be used to build heterometallic oligonuclear arrays.

1 Introduction

The metal ion-induced assembly of ligand molecules to give distinct structures is known as complex formation; Alfred Werners co-ordination theory[1] was the basis for a development that has led us to an understanding of the directionality of the interactions involving transition metal centers and of ways to design ligands that may be used to construct arrays of transition metal ions and ligand molecules with distinct topological features. Thus, self-assembly and self-organization processes that involve transition metal ions are often simple complex formation reactions, and the orientation of relatively rigid ligands around metal ions has been used extensively to produce co-ordination compounds with specific structural features.[2] Polytopic ligands have been designed to produce oligonuclear arrays with regular and aesthetically satisfying structures. Polypyridine-based ligands have been of particular importance, due to the photophysical properties of some of the corresponding transition metal complexes [specifically those of ruthenium(II)],[3,4] due to their increasing availability and to their

Peter Comba (born in 1953) obtained a diploma in chemistry and in chemical education from the ETH Zürich and a PhD from the Université de Neuchâtel [base hydrolysis of cobalt(III) pentaamines, Werner Marty]. He made preparative, structural and spectroscopic studies on transition metal hexaamine cage compounds with Alan Sargeson in Canberra and NMR studies on titanyl and decavanadate with André Merbach in Lausanne before setting up his own research group in Basel and later in Heidelberg. Two sabbaticals were used to start projects on single crystal spectroscopy and angular overlap model (AOM) calculations (with Michael Hitchman in Hobart) and on blue copper proteins (with Gerard Canters in Leiden). Peter's research is based on classical co-ordination chemistry with projects that range from bioinorganic chemistry (metalloproteins and model compounds) to structural, spectroscopic, electrochemical and mechanistic studies, and that also include applications such as metal ion selectivity and catalysis. New approaches to molecular modeling of inorganic compounds have been developed, and these are used extensively for the design of new compounds and for the determination of structures in solution.

Andreas Kühner (born in 1968) obtained his diploma and PhD from Heidelberg University. Currently, he has a position with Merck (Darmstadt). Andreas' main preparative achievements in Heidelberg were the development of a new method for the synthesis of tetrathiamacrocyclic ligands and the preparation of a series of new ligands with ferrocenyl end groups. He also developed a new molecular mechanics based approach for the quantification of the preorganization of macrocyclic ligands. Andreas' main scientific activity for his PhD in Peter's research group was the study of the solution structure and dynamics of the helical dicopper(I) compounds by NMR spectroscopy and molecular modeling.

Alexander Peters (born in 1969) obtained his diploma from Heidelberg Universtity and is now doing research work for his PhD thesis in Peter's group. Alex has done a beautiful mechanistic study on the ring contraction of tetrathiamacrocyclic ligands. He was involved in the synthesis of the ligands with the ferrocenyl end groups and also in structural studies on dicopper(II) compounds that included solid state structures, solution structures based on EPR spectra and molecular modeling. His main area of interest now is metal–metal interactions, and he develops ligand systems that bind $Ru^{II/III}$ *as well as* $Cu^{I/II}$.

Peter Comba

Andreas Kühner

Alexander Peters

rigidity and the emerging structural and molecular properties.[2,5,6] There is an increasing literature on molecular devices based on self-assembled ladders, grids, wires, metallacycles, polyhedra and helicates.[2,5–10] Metal ion-induced helicity, in particular, has attracted much attention because helicity is an important structural element in biological systems. The large majority of reported helicates is based on polypyridine derivatives,[11–22] and there are relatively few systems where the solution structural properties and the dynamic behavior have been studied in detail.[15] Exceptions include recent reports on helical titanium(IV) catecholate compounds[23] and on six-co-ordinated cobalt(II), nickel(II) and zinc(II) compounds of a macrocyclic Schiff base ligand.[24] In both of these examples solution NMR studies have been used to confirm the conservation of the observed solid state structural features, and temperature-dependent NMR studies have been used to analyse dynamic processes in solution.

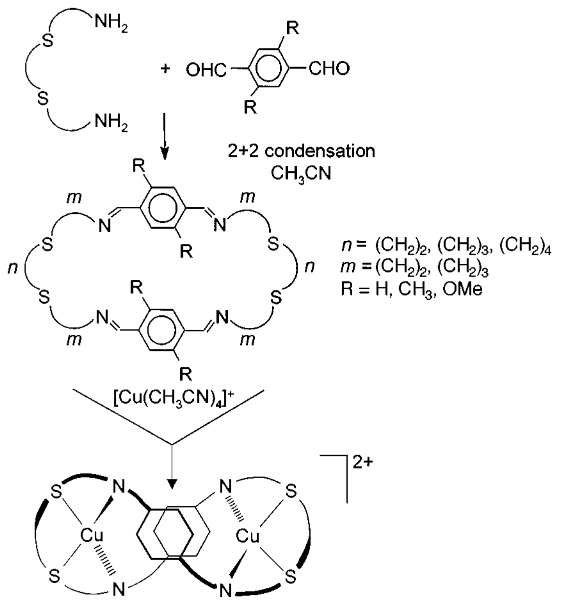

Chart 1

Recently, a new type of macrocyclic Schiff base compound with $(N_2S_2)_2$ (bis-dithiadiimine) donor sets has been reported which, upon co-ordination to two copper(I) ions, leads to double helical figure-of-eight shaped folding (see Chart 1).[25–29] The solid state structural properties of these dicopper(I) compounds have been studied as a function of the chelate ring sizes and the substitution pattern of the phenylene spacer groups (see Table 1).[28] A preorganized ligand, based on a tetrasubstituted paracyclophane anchor group, has also been prepared and studied for comparison (Table 1).[27] The solution structures and dynamics have been investigated with high-field and variable temperature ^{1}H NMR spectroscopy, respectively.[28] The experimentally determined isomer and conformer equilibria have been compared to the computed ratios based on force field calculations.[29] The mechanisms for the isomerization and racemization processes are discussed on the basis of the observed and the computed data, and these have some implication on the understanding of the redox stability of these compounds and on the stereochemistry and dynamics of other compounds in the areas of supramolecular and biological systems. Folded macrocyclic structures are also observed in some cyclic peptides (*e.g.* Cyclosporin A, Ascidiacylamide, Patellamide D) and their metal complexes.[30–34] The unique properties of these macrocycles and their metal complexes, occurring in bacteria, fungi, plants and marine organisms, have been related to the folding of the macrocyclic rings, and the results of our figure-of-eight-twisted system might have some implication in that area.

Table 1 Nomenclature of the ligands

Name	$m^{a,b}$	n^a	spacer^b
para-222	$(CH_2)_2$	$(CH_2)_2$	1
para-222-Me	$(CH_2)_2$	$(CH_2)_2$	2
para-222-OMe	$(CH_2)_2$	$(CH_2)_2$	3
para-phane-222	$(CH_2)_2$	$(CH_2)_2$	6
para-Ph2Ph	5	$(CH_2)_2$	1
para-232	$(CH_2)_2$	$(CH_2)_3$	1
para-242	$(CH_2)_2$	$(CH_2)_4$	1
para-323	$(CH_2)_3$	$(CH_2)_2$	1
para-333	$(CH_2)_3$	$(CH_2)_3$	1
meta-222	$(CH_2)_2$	$(CH_2)_2$	4

[a] See Chart 1. [b] Spacer groups (1)–(6) are shown below.

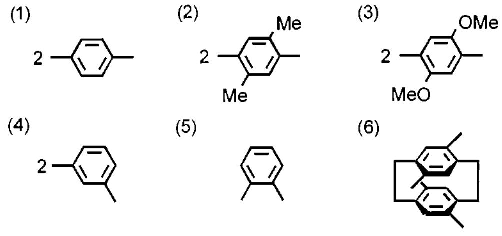

Table 2 Structural parameters (bond lengths in Å, angles in °) of the chromophores of the dicopper(I) compounds of Fig. 1

	para-222	meta-222	phane-222
Cu–S	2.38(2)	2.43(1)	2.38(2)
Cu–N	2.01(8)	1.99(1)	1.96(1)
Cu···Cu	7.83	8.15	8.22
S–Cu–S	91.0(4)	88.2	91.51(2)
S–Cu–N	115.1(37)	113.3(24)	117.4(14)
S–Cu–N^{bite}	90.8(18)	89.7(6)	90.2(6)
N–Cu–N	144.1(42)	148.5	141.2(1)

2 Solid state structures

The structure of the molecular cation of the dicopper(I) compound of the helically preorganized ligand with the paracyclophane anchor group (phane-222, see Table 1), based on X-ray crystallography, is shown in Fig. 1.[27] The copper(I)–donor distances and the valence angles around the metal centers and the donor groups (see Table 2 for the relevant structural data) are as expected for this type of co-ordination compound, that is the observed geometry is relatively unstrained and, therefore, the paracyclophane anchor group might not be required for the folding to a figure-of-eight shaped geometry of this type of ligand. Indeed, the geometry of the dicopper(I) product of the large macrocyclic ligand para-222 (32-membered macrocycle), whose experimental structure is also given in Fig. 1,[26] is very similar: the main and expected differences are a decrease in the distance between the aromatic rings for the paracyclophane derivative, due to the ethylene bridges, and a concomitant small increase in the copper(I)–copper(I) distance (see Table 2). Thus, a preorganization with the synthetically demanding paracyclophane anchor group is not required for the helical figure-of-eight shaped folding.

An interesting feature is that copper(I) induced folding of the isomer of para-222 with *meta*- instead of *para*-phenylene spacer groups, meta-222 (30- instead of 32-membered macrocycle), leads to a similar shape of the ligand backbone [the experimental structure of the dicopper(I) compound of meta-222 is also presented in Fig. 1].[26] The copper(I) co-ordination geometries, the copper(I)–copper(I) distances and the relative orientation of the two aromatic rings are very similar (see also Table 2) but the $[Cu_2(meta\text{-}222)]^{2+}$ structure is achiral ("squeezed" instead of "twisted" macrocyclic ring, see Chart 2). All other

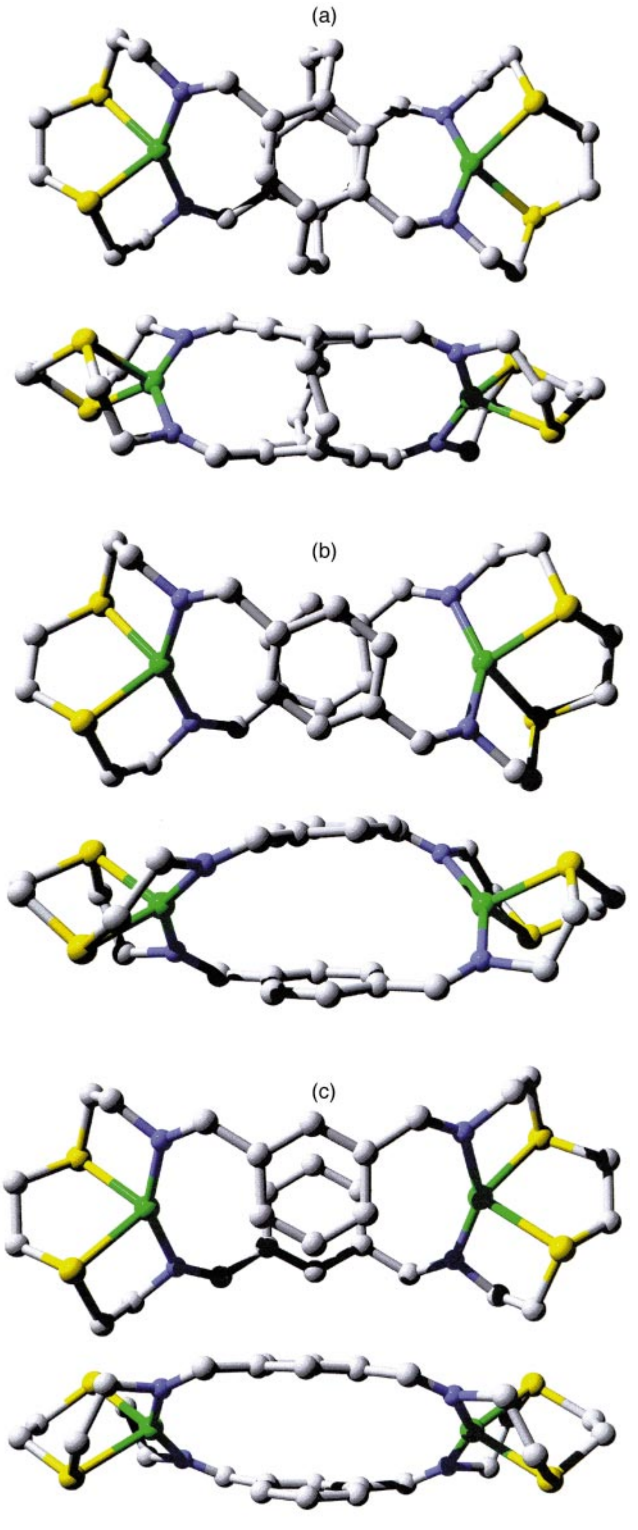

Fig. 1 Plots of the experimentally determined (X-ray) structures of the molecular cations of (a) [Cu$_2$(phane-222)]$^{2+}$,[27] (b) [Cu$_2$(para-222)]$^{2+}$ [26] and (c) [Cu$_2$(meta-222)]$^{2+}$.[26]

ligand modifications lead to species that show copper(I) induced helicity [note that increasing thiaether–imine chelate ring sizes lead to instability of the dicopper(I) products, see below]. The structures of all helicates, based on macrocyclic ligands, that have been determined experimentally are assembled in Fig. 2 and the relevant structural data are summarized in Table 3. The only significant structural variations are those of the valence angles that involve the metal centers, and these are due to the changes in the chelate ring sizes.

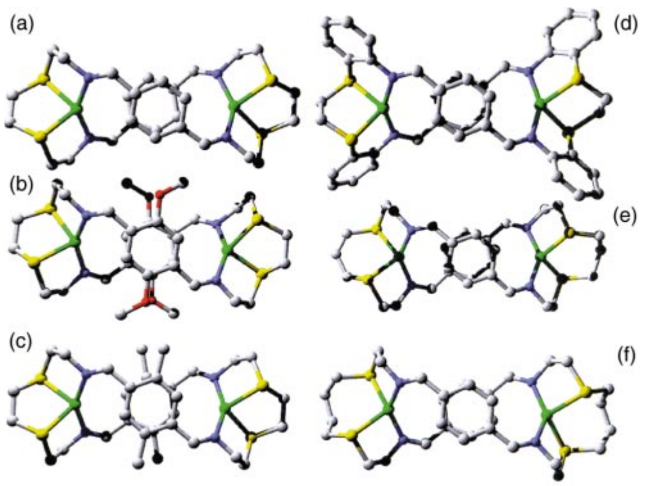

Fig. 2 Plots of the experimentally determined (X-ray) structures of the molecular cations of (a) [Cu$_2$(para-222)]$^{2+}$,[26] (b) [Cu$_2$(para-222-OMe)]$^{2+}$,[28] (c) [Cu$_2$(para-222-Me)]$^{2+}$,[28] (d) [Cu$_2$(para-Ph2Ph)]$^{2+}$,[25] (e) [Cu$_2$(para-232)]$^{2+}$ [28] and (f) [Cu$_2$(para-242)]$^{2+}$.[28]

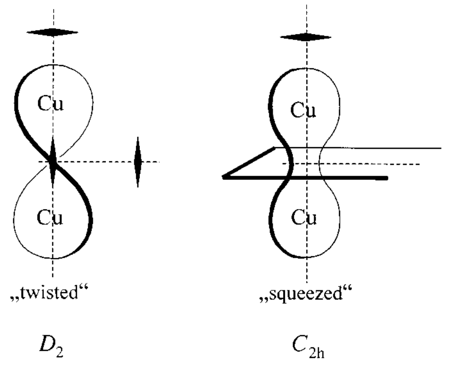

Chart 2

For the helicates there are three sources of chirality: the helicity, based on the backbone of the co-ordinated macrocycle (Λ or Δ), the configuration of the co-ordinated thioether donors (S* or R*) and the conformation of the chelate rings (λ or δ for five-membered chelate rings). Since the assignment of the configuration of the co-ordinated thioether-S donor groups depends on the ligand structure (chelate ring sizes), we use a generalized nomenclature (S'* or R'*) which is based on the ligand with ethylene bridges between all donor groups of each co-ordination site (para-222), that is the priorities [Cahn–Ingold–Prelog (CIP) rules] are $\mathrm{Cu^+ > C_{thiaether} > C_{imine}}$ > lone pair.

All structurally characterized helicates crystallize in racemic point groups, and all structures have the same configuration, that is $\Delta R'^*R'^*R'^*R'^*$ or $\Lambda S'^*S'^*S'^*S'^*$ (for species with five-membered chelate rings the corresponding conformations are δ and λ for the thioether-S configurations R'* and S'*, respectively; *e.g.* $\Delta R'^*R'^*R'^*R'^*\delta\delta\delta\delta\delta\delta$). The exclusive observation of a single isomer out of 350 non-degenerate diastereomeric possibilities in the solid state indicates that this might be considerably more stable than all the others. Support for this assumption emerges from force field calculations[29] and from the investigation of the solution structures and dynamics (see below). From the fact that only one isomer is observed, that is that all stereocenters are strongly coupled, it follows that the structure of the *co-ordinated* ligand is rather rigid. Thus, the folded structures might be retained in solution and dynamic processes might be slower than anticipated and possibly detectable by NMR spectroscopy (the rate of interconversion of five-membered chelate rings is generally of the order of 10^8 s^{-1} [35,36] and water exchange at copper(I) is of the order of 10^{10} s^{-1} [37]). It also follows that the figure-of-eight shaped structures are probably due to the tetrahedral co-ordination geometry, enforced by

Table 3 Average distances (Å) and angles (°) of all figure-of-eight-shaped dicopper(II) compounds with $(N_2S_2)_2$ donor sets

	para-222	para-222-Me	para-222-OMe	para-Ph2Ph	para-232	para-242	meta-222	phane-222
Cu–S	2.38(2)	2.40(6)	2.40(2)	2.34(4)	2.35(3)	2.41(2)	2.43(1)	2.38(2)
Cu–N	2.01(8)	1.98(1)	1.98(2)	2.00(2)	2.02(3)	2.02(2)	1.99(1)	1.96(1)
Cu···Cu	7.83	7.70	7.86	7.77	7.95	8.14	8.15	8.22
$C^{benz}\cdots C^{benz}$	3.43	3.57	3.53	3.42	3.42	3.45	3.26; 3.43	—
benz···benz	3.59	3.55	3.56	3.45	3.49	3.57	3.39	3.09
S–Cu–S	91.0(4)	90.2	90.3(6)	93.1(2)	102.6(34)	103.6(9)	88.2	91.51(2)
S–Cu–N	115.1(37)	114.1(25)	114.8(57)	113.2(22)	116.4(66)	118.8(80)	113.3(24)	117.4(14)
$S–Cu–N^{bite}$	90.8(18)	89.4(6)	89.7(12)	88.0(2)	90.2(2)	88.5(12)	89.7(6)	90.2(6)
N–Cu–N	144.1(42)	147.2	145.4(3)	149.8(4)	138.1(17)	136.1(8)	148.5	141.2(1)
$C^{imine}–C^{benz\,a}$	31	29	33	23	25	28	27	32
θ^b	73	72	73	72	73	72	73	71
φ^c	16	14	13	17	19	13	—	—

[a] Torsional angle around the imine bond. [b] Tetrahedral twist angle (S–Cu–S; N–Cu–N planes; tetrahedral: 90°). [c] Torsional angle about the centroids of the benzene spacer groups.

the copper(I) centers. Although the aromatic spacer groups are ideally π-stacked, the resulting stabilization is probably not decisive for the enforcing of the figure-of-eight geometry.[28] From the rigidity of the co-ordinated ligand it follows also that co-ordination to copper(I) is entropically an unfavorable process. That is, the gain in complex stability by the preorganization of the ligand (phane-222) should be appreciable.

3 Structures in solution

Proton NMR spectroscopy indicates that the metal-free ligands are not preorganized (that is they have a flexible, macrocyclic structure) and that the figure-of-eight shaped folding of the dicopper(I) complexes is retained in solution when an inert solvent (*e.g.* nitromethane) is used.[25–28] In the simplest example for ^{1}H NMR spectroscopy, that of para-Ph2Ph, which has only one type of methylene proton, there is one sharp singlet for these protons in the metal-free ligand. In the helical dicopper(I) compound these become diastereotopic and give rise to a four line AX system at 200 MHz, with a geminal coupling of 10.5 Hz and a chemical shift difference of $\Delta\delta = 1.5$ ppm (the vicinal coupling that would give rise to an AA′XX′ pattern is not observed).[25] The observation that the metal-free ligands are unfolded supports the assumption that the π-stacking interaction is not strong and is not the main driving force for the figure-of-eight shapes (see above). For three of the double helical dinuclear compounds [the dicopper(I) compounds of para-222, para-242 and para-222-OMe] the solution structures have been determined by high resolution ^{1}H NMR spectroscopy in nitromethane.[28] The spectrum of $[Cu_2(para\text{-}222)]^{2+}$ (aliphatic region) is shown in Fig. 3 and the nomenclature of the protons is given in Chart 3. The assignment of the signals is based on two dimensional homonuclear (^{1}H–^{1}H)- and heteronuclear (^{1}H–^{13}C)-correlated spectra, and the coupling patterns (see Fig. 3) are based on a first-order analysis.

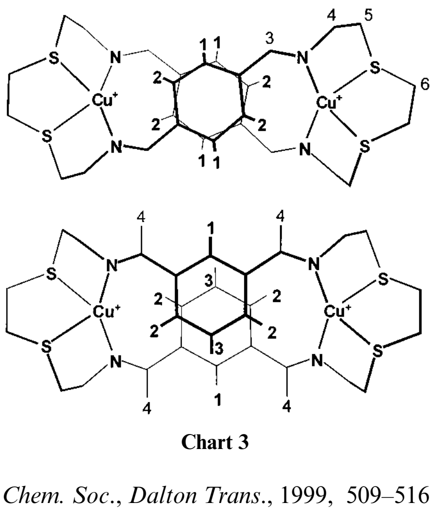

Chart 3

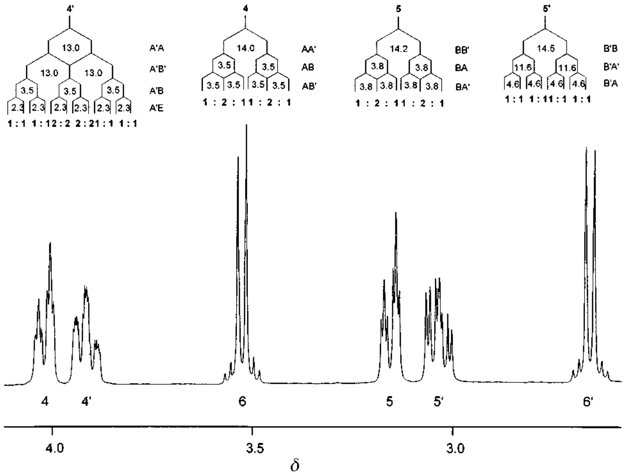

Fig. 3 Proton NMR spectrum (500 MHz) of $[Cu_2(para\text{-}222)]^{2+}$ (high field region).[28]

In the region of aromatic protons there should be two doublets for the structurally different protons of the *para*-phenylene spacer groups (see Chart 3). The fact that only one singlet was observed indicates that a dynamic process is involved which interconverts the two sites.[28] A helix inversion with full retention of the co-ordinative bonds corresponds to an epimerization, that is to an equilibrium between two diastereomers, *e.g.* $\Lambda S'*S'*S'*S'* \rightleftharpoons \Delta S'*S'*S'*S'*$ (see sections on conformational analysis and on dynamics, below; the rigidity of the co-ordinated ligands, discussed above, implies that both diastereoisomers have distinct and possibly different sets of five-membered chelate ring conformations).

For the achiral dicopper(I) compound of meta-222 the expectation is that in the low field region of the ^{1}H NMR spectrum there is a singlet for the imine proton (double intensity), and a singlet, a doublet (double intensity) and a triplet for the three distinct aromatic protons (see Chart 3). The observed spectrum (Fig. 4) indicates that two isomers in a ratio of approximately 1 : 3 are present.[29] While one of them probably is that observed in the solid (see Fig. 1; tail-to-tail isomer), the other may correspond to one of the other two structures that result from a rotation of the phenylene spacer groups around the C_{aromat}–C_{imine}–bonds (Chart 4). Note that the tail-to-tail and head-to-head isomers both have C_{2h} symmetry while that of the head-to-tail isomer is C_s. That is, the head-to-tail isomer should have two sets of signals for protons 1, 2 and 3, and a possible conclusion is that the two isomers present in solution are tail-to-tail and head-to-head.

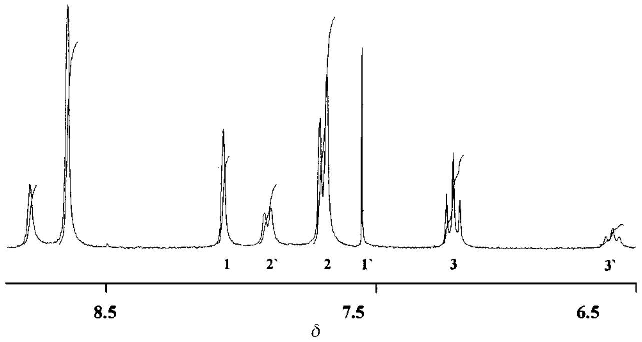

Fig. 4 Proton NMR spectrum (200 MHz) of $[Cu_2(meta\text{-}222)]^{2+}$ (low field region).[29]

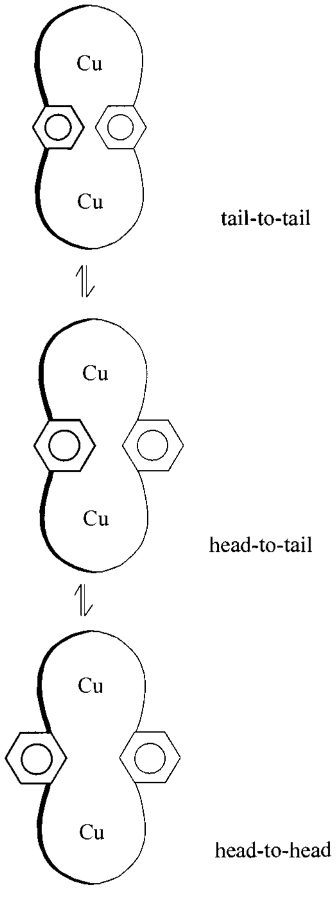

Chart 4

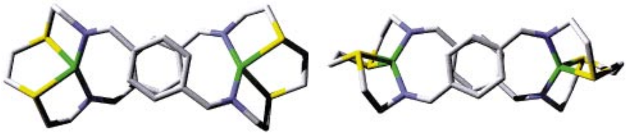

Fig. 5 Computed structures[29] of the helix inversion products of $[Cu_2(para\text{-}222)]^{2+}$ with conserved thioether-S configurations (Δ-$R'*R'*R'*R'*$-δδδδδδ $\rightleftharpoons$ Λ-$R'*R'*R'*R'*$-δδδδδδ).

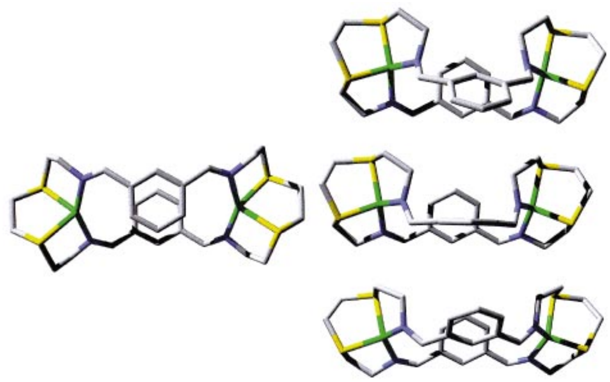

Fig. 6 Computed structures[29] of the tail-to-tail (head-to-tail) conversion products of $[Cu_2(meta\text{-}222)]^{2+}$ showing the three low-energy structures of the head-to-tail rotamer.

4 Conformational analysis

Empirical force field calculations have been used extensively for predictions of conformational equilibria.[38–40] The MOMEC force field is mainly based on structural experimental data but there are good reasons to believe that the steepness of the potentials is approximately realistic, that is the isomer ratios are well represented by the relative strain energies[41–43] and this has been tested extensively.[40–45] The two isomers $[Cu_2(para\text{-}222)]^{2+}$ and $[Cu_2(meta\text{-}222)]^{2+}$ (ethylene bridges between all donor atoms) were analysed in detail.[29] For the isomer with *para*-substituted spacer groups the geometry observed in the solid, that is Λ-$S'*S'*S'*S'*$-λλλλλλ-$[Cu_2(para\text{-}222)]^{2+}$, is the most stable structure (0 kJ mol^{-1}). The destabilization due to an inversion of a five-membered chelate ring is approximately 5 kJ mol^{-1}; that due to an inversion of a thioether-S donor is approximately 16 kJ mol^{-1}. Obviously, these effects are not additive (that is for each configuration there is a preferred set of conformations). The next lowest energy structure (five-membered ring inversions alone excluded; inversion barriers of five-membered chelate rings are approximately 25 kJ mol^{-1},[35,36] that is their interconversion will not be frozen, even at low temperature) is that of the helix inversion product, Δ-$S'*S'*S'*S'*$-λλλλλλ-$[Cu_2(para\text{-}222)]^{2+}$, with a strain energy of 6 kJ mol^{-1} (Fig. 5).

Only two of the three putative isomers of $[Cu_2(meta\text{-}222)]^{2+}$ from Chart 4 converge to a stable structure. The lowest energy structure is tail-to-tail-$R'*R'*S'*S'*$-δδδλλλ-$[Cu_2(meta\text{-}222)]^{2+}$ (12 kJ mol^{-1}), that is the geometry observed in the crystal.[26] Inversion of thioether-S donors and five-membered chelate rings leads to destabilizations of the same order of magnitude as for the isomers with the *para*-phenylene spacer groups. The lowest energy conformer of the head-to-tail rotamer, $R'*R'*S'*S'*$-λδλδλλ-$[Cu_2(meta\text{-}222)]^{2+}$, is approximately 7 kJ mol^{-1} less stable than the lowest energy tail-to-tail isomer.[29] No energy minimum could be detected for the head-to-head rotamer. There are two interesting features emerging from the strain energy minimized head-to-tail rotamer (see Fig. 6). (i) The two *meta*-phenylene rings are tilted with respect to each other. (ii) There is a shallow energy surface with at least three minima with similar energies and energy barriers of less than approximately 25 kJ mol^{-1}, that is there is a wagging mode of the two spacer groups.

Both observations are consistent with the observed ^1H NMR spectrum (Fig. 4): the observed ratio of isomers of approximately 3 : 1 is in agreement with a strain energy difference of *ca.* 7 kJ mol^{-1}. The fast dynamics in the head-to-tail isomer that involves three orientations of each of the *meta*-phenylene spacer groups is consistent with the observation of single sets of singlets, doublets and triplets for the aromatic protons. The chemical shift differences between the metal-free meta-222 ligand and the major isomer (tail-to-tail) and those between the major and the minor species in the ^1H NMR spectrum of Fig. 4 (tail-to-tail and head-to-tail) were interpreted with a tilt of the two aromatic rings, and that is in agreement with the computed structures (Fig. 6).[28,29]

5 Dynamics

For the helical dicopper(I) compounds there are two dynamic processes: (i) a low temperature (coalescence at approximately 220 K) solvent independent process assigned to helix inversion

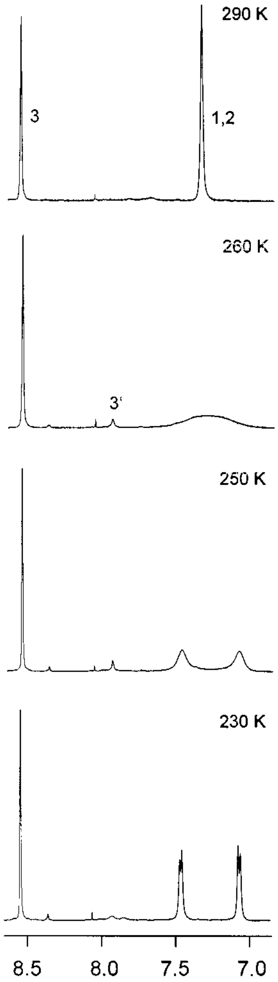

Fig. 7 Temperature dependent 500 MHz ^{1}H NMR spectra of [Cu_2-(para-242)]$^{2+}$ (low field region).[28]

with retention of the thioether-S configurations, that is epimerization that involves Λ-$S'*S'*S'*S'*$- and Δ-$S'*S'*S'*S'*$-[Cu_2(para-222)]$^{2+}$; (ii) a high temperature (coalescence at approximately 300 K) process in acetonitrile attributed to full racemization (helix inversion and scrambling at all thioether-S donors).[28] The former process is observed in the low field region of the ^{1}H NMR spectrum. Each of the two diastereoisomers (ratio of approximately 92 : 8, based on the strain energy difference of 6 kJ mol^{-1}) is expected to have a singlet for the imine protons and two doublets for the aromatic protons (exception: species with substituted *para*-phenylene spacer groups, see below). The ambient temperature ^{1}H NMR spectra of all helicates have two singlets (ratio 1 : 2) in the low field area of the spectrum (see Fig. 7). At the lowest possible temperature, the signal for the aromatic protons of [Cu_2(para-242)]$^{2+}$ splits into two doublets. The signals of the aromatic protons of the less abundant isomer could not be resolved. However, a small signal (see 3′ in Fig. 7; this signal was reproduced in various samples) may be attributed to the resonance of the imine protons of the less abundant diastereoisomer.[28] The high-field shift is consistent with the expected change of the torsion around the imine bond.[28,29]

The high temperature dynamics process (high field region of the ^{1}H NMR spectrum, see Fig. 8), attributed to full racemization, is only observed in acetonitrile which has a high affinity for copper(I). This and the fact that the activation barrier for this process is significantly higher suggest that some bond breaking might be involved. That is, there are intermediates where acetonitrile is co-ordinated to the copper(I) centers. Crystals of such a putative intermediate could be isolated and structurally characterized (Fig. 9).[28]

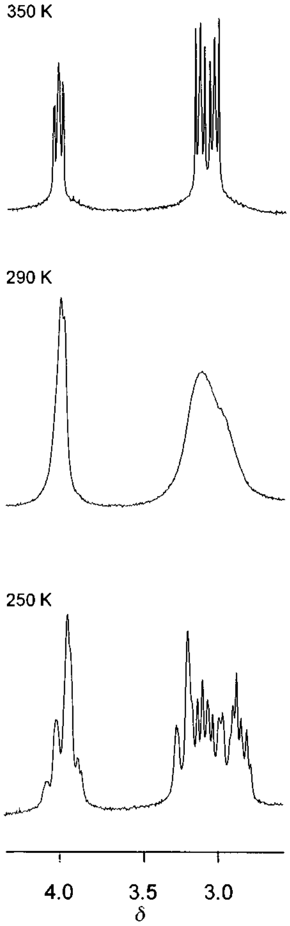

Fig. 8 Temperature dependent 200 MHz ^{1}H NMR spectra of [Cu_2-(para-232)]$^{2+}$ (high field region).[28]

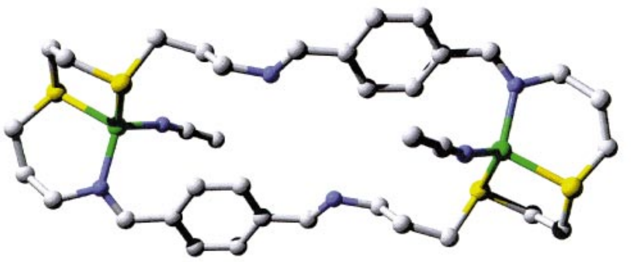

Fig. 9 Plot of the experimentally determined (X-ray) structure of the molecular cation of [Cu_2(para-323)(CH_3CN)$_2$]$^{2+}$.[28]

The coalescence temperature of the two compounds with substituted *para*-phenylene bridges is approximately 50 K higher than for all the other helicates (approximately 320 *vs.* approximately 270 K).[28] A possible explanation is that acetonitrile exchange is activated along the helix inversion reaction coordinate, a process that is disfavoured by the *para*-phenylene substitution (see Chart 5). This is supported by strain energy minimized structures along the helix inversion coordinate (constrained pseudo-torsional angle that involves the two *para*-phenylene centroids) that indicate that the *para*-phenylene–*para*-phenylene distance increases from approximately 3.3 to approximately 4.9 Å at the transition state of the inversion reaction.[29] The distortions along the helix inversion reaction coordinate also indicate that there is a low energy rotation of the *para*-phenylene rings along this mode, and this is consistent with the ^{1}H NMR data. The computed activation barrier of approximately 50 kJ mol^{-1} is qualitatively in agreement with the barrier emerging from the ^{1}H NMR experiments.[29]

The dynamics of the “squeezed ring” isomer [Cu_2(meta-

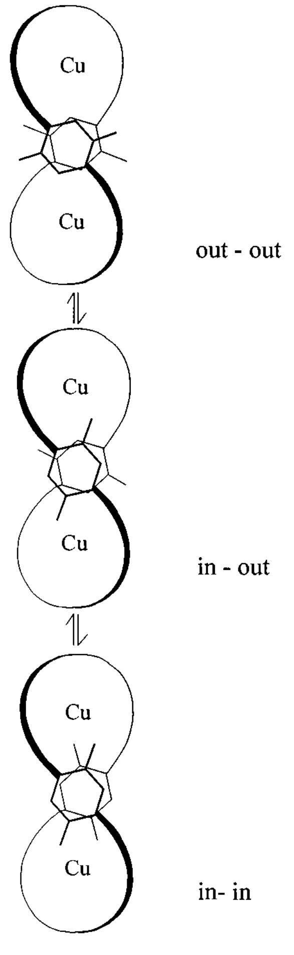

Chart 5

222)]$^{2+}$ is strikingly different: (i) only one process has been observed, and, based on ^{1}H NMR spectroscopy, it is attributed to full scrambling, that is it involves copper–donor bond breaking; (ii) this process is solvent dependent but it also occurs in nitromethane (coalescence temperature: in acetonitrile, 250 K; in nitromethane, 330 K).[29] This is interpreted to be due to a more dissociative character of the scrambling process than for the helicates, and this interpretation is supported by force field calculations and the general observation that the "squeezed ring" isomer is considerably less stable than the "twisted ring" compounds (activation of the oxygenation reaction along the intramolecular dynamic process).[29]

6 Extensions

The preparative concepts used for the ligands that lead to helical and "squeezed ring" figure-of-eight shaped dicopper(I) compounds have been extended to include a variety of aldehydes and amines (Chart 6). The combination of the di- or tetra-aldehydes **1**–**3** with dithiadiamines **6** leads to Schiff-base ligands that form figure-of-eight shaped dicopper(I) compounds.[25–29] Similar ligands may be isolated in good yields when dialdehydes of the type **4** are used (nomenclature of the resulting ligands: 222-S_4, 222-S_6, 222-S_8, for $n = 0, 1, 2$, respectively). The structures of the corresponding tricopper(I) compounds $[Cu_3(222\text{-}S_4)]^{3+}$, $[Cu_3(222\text{-}S_6)]^{3+}$ and $[Cu_3(222\text{-}S_8)]^{3+}$ were characterized by elemental analysis, ^{1}H NMR, ESI-MS and IR spectroscopy. Proton NMR spectroscopy was used to analyse the binding mode of the copper(I) ion that is co-ordinated to the central S_4, S_6 or S_8 donor group. In acetonitrile and in nitromethane there is formation of C_{2v}-symmetric complex cations. The resonances attributed to the two peripheral dithiadiimine donor sets are similar to those of the dicopper(I) helicates. Thus the corresponding two copper(I) ions are tetrahedrally co-ordinated but, based on the ^{1}H NMR chemical shift data of the *para*-phenylene groups, there is no π stacking of the

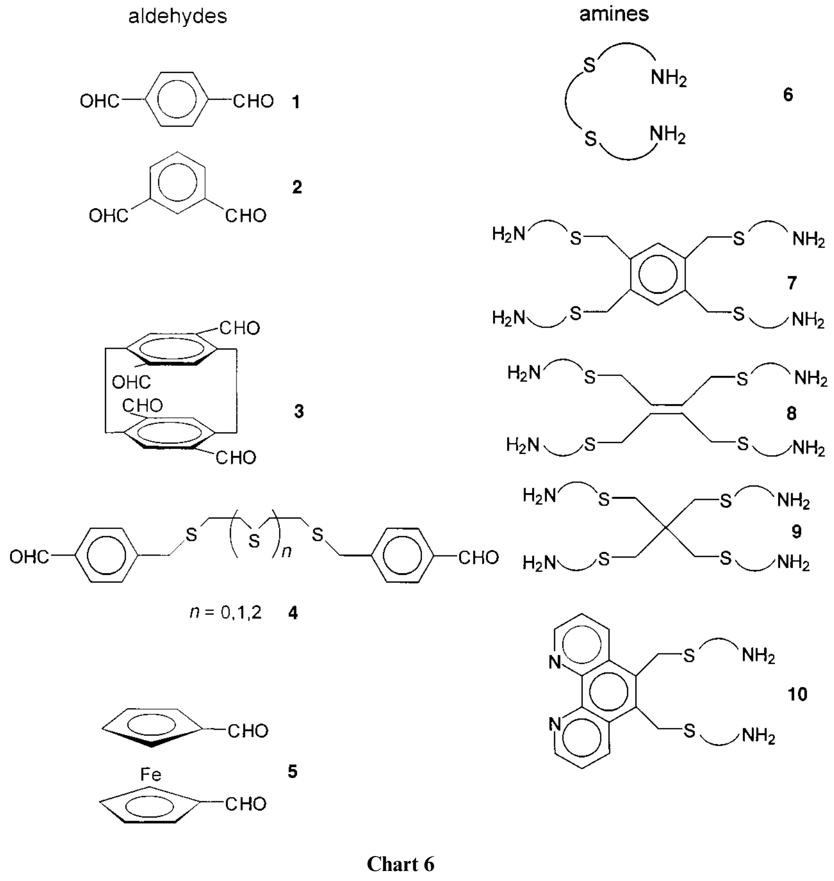

Chart 6

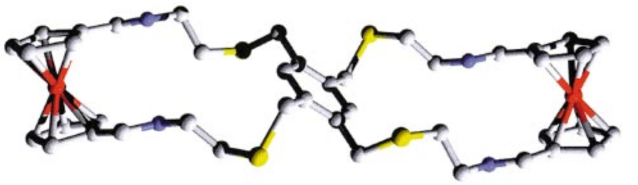

Fig. 10 Plot of the experimentally determined (X-ray) structure of the ligand based on two ferrocenyl end groups and the tetraamine **7**.[47]

aromatic spacer groups.[28] The downfield shifts of the ethylene bridges in the central S_4, S_6 or S_8 binding sites upon co-ordination to copper(I) are in the range that usually is observed for co-ordinated thioether macrocyclic ligands.[46] These chemical shifts indicate that the third copper(I) center is co-ordinated in the central cavity. For $[Cu_3(222\text{-}S_6)]^{3+}$ there is a fast dynamic process that leads to an average co-ordination mode that makes all six thioether donors identical. In $[Cu_3(222\text{-}S_8)]^{3+}$ the co-ordination of the central copper(I) ion involves only the four central thioether donors.

The [2 + 1] condensation of 1,1′-bis(formyl)ferrocene **5** with the tetrathiatetraamines **7**–**9** leads to ligands with two ferrocenyl end-groups and two sites for metal ion co-ordination. The structure of the bis(ferrocenyl) "free" ligand and the corresponding dicopper(I) compound, based on **7**, have been determined by X-ray crystallography and ^{1}H NMR spectroscopy, respectively. For **7** and **8** there are two isomers, and both were observed by ^{1}H NMR spectroscopy of the copper(I)-free ligands. The isomer that crystallized (Fig. 10) does not lead to stable dicopper(I) compounds, and this also emerged from ^{1}H NMR spectroscopy. The metal–metal interactions in the dicopper(I) compounds have been studied by electrochemistry, IR and Mössbauer spectroscopy.[47]

Of particular interest is the bifunctional diamine building block **10** which recently has been isolated and characterized. This allows the combination of the chemistry of the helicates discussed here with ruthenium–phenanthroline type co-ordination chemistry. Together with the ferrocenyl and the tris(phenanthroline) ruthenium end-groups, based on **5** and **10**, there is now the possibility to assemble helicates and arrays of helicates with photochemically and/or electrochemically active sites.

7 Acknowledgements

Generous financial support by the Deutsche Forschungsgemeinschaft (DFG) and the Fond der Chemischen Industrie (FCI) is gratefully acknowledged.

8 References

1 A. Werner, *Z. Anorg. Allg. Chem.*, 1893, **3**, 271.
2 J.-M. Lehn, *Supramolecular chemistry concepts and perspectives*, VCH, Weinheim, 1995.
3 A. Juris, V. Balzani, F. Barigelletti, S. Campagna, P. Belser and A. von Zelewsky, *Coord. Chem. Rev.*, 1988, **84**, 85.
4 F. Scandola, M. T. Indelli, C. Chiorboli and C. A. Bigmozzi, *Top. Curr. Chem.*, 1990, **158**, 73.
5 E. C. Constable, *Adv. Inorg. Chem. Radiochem.*, 1987, **30**, 69.
6 V. Balzani and F. Scandola, *Supramolecular Photochemistry*, Ellis Horwood, Chichester, 1991.
7 S. Mann, G. Huttner, L. Zsolnai and K. Heinze, *Angew. Chem.*, 1996, **108**, 2983.
8 B. Hasenknopf, J. M. Lehn, B. O. Kneisel, G. Baum and D. Fenske, *Angew. Chem.*, 1996, **108**, 1987.
9 P. N. W. Baxter, G. S. Hanan and J. M. Lehn, *Chem. Commun.*, 1996, 2019.
10 A. Harriman and R. Ziessel, *Chem. Commun.*, 1996, 1707.
11 E. C. Constable, *Nature* (*London*), 1990, **346**, 314.
12 J.-P. Sauvage, *Acc. Chem. Res.*, 1990, **23**, 319.
13 J.-M. Lehn, *Angew. Chem.*, 1990, **102**, 1347.
14 E. C. Constable, *Chem. Ind.*, 1994, 56.
15 C. Piguet, G. Bernardinelli and G. Hopfgartner, *Chem. Rev.*, 1997, **97**, 2005.
16 U. Koert, M. M. Harding and J.-M. Lehn, *Nature* (*London*), 1990, **346**, 339.
17 W. Zarges, J. Hall and J.-M. Lehn, *Helv. Chim. Acta*, 1991, **74**, 1843.
18 J. K. Judice, S. J. Keipert and D. J. Cram, *J. Chem. Soc.*, *Chem. Commun.*, 1993, 1323.
19 K. T. Potts, M. Keshavarz, F. S. Tham, H. D. Abruna and C. Arana, *Inorg. Chem.*, 1993, **32**, 4436.
20 R. Krämer, J.-M. Lehn and A. DeCian, *Angew. Chem.*, 1993, **105**, 764.
21 E. C. Constable, A. J. Edwards, P. R. Raithby and J. V. Walker, *Angew. Chem.*, 1993, **105**, 1486.
22 A. Bilyk and M. M. Harding, *J. Chem. Soc.*, *Dalton Trans.*, 1994, 77.
23 M. Albrecht, *Chem. Eur. J.*, 1997, **3**, 1466.
24 D. E. Fenton, R. W. Matthews, M. McPartlin, B. P. Murphy, I. J. Scowen and P. A. Tasker, *J. Chem. Soc.*, *Chem. Commun.*, 1994, 1391.
25 P. Comba, A. Fath, T. W. Hambley and D. T. Richens, *Angew. Chem.*, 1995, **107**, 2047.
26 P. Comba, A. Fath, T. W. Hambley and A. Vielfort, *J. Chem. Soc.*, *Dalton Trans.*, 1997, 1691.
27 P. Comba, A. Fath, G. Huttner and L. Zsolnai, *Chem. Commun.*, 1996, 1885.
28 P. Comba, A. Fath, T. W. Hambley, A. Kühner, D. T. Richens and A. Vielfort, *Inorg. Chem.*, 1998, **37**, 4389.
29 P. Comba and A. Kühner, *Eur. J. Inorg. Chem.*, 1998, accepted.
30 J. P. Michael and G. Pattenden, *Angew. Chem.*, 1993, **105**, 1.
31 J. R. Lewis, *Nat. Prod. Rep.*, 1989, **6**, 503.
32 H. C. Krebs, *Fortschr. Chem. Org. Naturst.*, 1986, **49**, 151.
33 D. P. Fairlie, G. Abbenante and D. M. March, *Curr. Med. Chem.*, 1995, **2**, 672.
34 P. Comba, R. Cusack, D. P. Fairlie, L. R. Gahan, G. R. Hanson, U. Kazmaier and A. Ramlow, *Inorg. Chem.*, 1998, in the press.
35 T. W. Hambley, *J. Comput. Chem.*, 1987, **8**, 651.
36 Y. Kuroda, N. Tanaka, M. Goto and T. Sakai, *Inorg. Chem.*, 1989, **28**, 997.
37 Y. Ducommun and A. E. Merbach, *Inorganic High Pressure Chemistry*, *Kinetics and Mechanisms*, ed. R. van Eldik, Elsevier, Amsterdam, 1986.
38 G. R. Brubaker and D. W. Johnson, *Coord. Chem. Rev.*, 1984, **53**, 1.
39 R. D. Hancock, *Prog. Inorg. Chem.*, 1989, **37**, 187.
40 P. Comba, *Coord. Chem. Rev.*, 1993, **123**, 1.
41 P. Comba and T. W. Hambley, *Molecular Modeling of Inorganic Compounds*, VCH, Weinheim, 1995.
42 P. Comba, in *Implications of Molecular and Materials Structure for New Technologies*, eds. J. K. A. Howard and F. H. Allen, Kluwer, Dordrecht, in the press.
43 P. Comba, *Coord. Chem. Rev.*, 1998, in the press.
44 P. Comba, in *Molecular Modeling and Dynamics of Bioinorganic Compounds*, eds. L. Banci and P. Comba, Kluwer, Dordrecht, Boston, 1997, p. 21.
45 J. E. Bol, C. Buning, P. Comba, J. Reedijk and M. Ströhle, *J. Comput. Chem.*, 1998, **19**, 512.
46 P. Comba, A. Fath, A. Kühner and B. Nuber, *J. Chem. Soc.*, *Dalton Trans.*, 1997, 1889.
47 P. Comba, A. Kühner and A. Peters, submitted for publication.

Paper 8/06075D